Korean J. Chem. Eng., **23**(4), 547-554 (2006)

Thermodynamic features of the Cu-ZSM-5 catalyzed NO decomposition reaction

Deuk Ki Lee†

Department of Environmental Engineering, Gwangju University, Gwangju 503-703, Korea
(*Received 30 August 2005 • accepted 23 February 2006*)

Abstract−Over a Cu-ZSM-5 catalyst with a quantified amount of the active Cu^{2+}-dimers (Cu^{2+}-O^{2-}-Cu^{2+}), the kinetics of the catalytic NO decomposition to N_2 and O_2 was derived on the basis of the proposed reaction mechanism, and such thermodynamic data as adsorption enthalpies of NO and O_2 onto the Cu ion dimer sites were evaluated. It was revealed that the enthalpy of the adsorption of NO (ΔH=−34.1 kcal/mol) onto a reduced Cu^{+}-dimer, as the initiating step of NO decomposition catalysis, was higher than that (ΔH=−27.8 kcal/mol) onto an oxidized Cu^{2+}-dimer, or that (ΔH=−27.4 kcal/mol) of the dissociative adsorption of O_2 onto the two reduced Cu^{+}-dimers in neighbor. The strong inhibition effect of gas phase oxygen on the kinetic rate of NO decomposition at 400-600 °C could be explained by the thermodynamic predominance of the oxidized Cu^{2+}-dimers against the active reduced Cu^{+}-dimers on the catalyst even at high temperature and under the low partial pressure of oxygen. It was also found that the maximum catalytic activity at temperatures around 500 °C, which was commonly observed in the Cu-ZSM-5 catalyzed NO decomposition reaction, was attributed to the relatively large enthalpy of NO adsorption onto the reduced Cu^{+}-dimers as compared to that of the reaction activation energy (=19.5 kcal/mol), resulting in less favored NO adsorption at the higher temperatures than 500 °C.

Key words: NO Decomposition, Cu-ZSM-5, Cu-dimers, Mechanism, Kinetics, Enthalpy of Adsorption, Activation Energy, Thermodynamics

INTRODUCTION

Irrespective of the extensive studies for more than a couple of decades, the direct decomposition of NO to N_2 and O_2 on Cu-ZSM-5 catalyst is still a very interesting topic in such fundamental respects as the identification of catalytic active sites and the elucidation of reaction mechanism leading to N_2 and O_2 formation in relation to the reaction kinetics. As summarized by Kuroda and Iwamoto [2004] or by Groothaert et al. [2003], it is generally accepted that atomic oxygen-bridged Cu^{2+}-dimer ions, Cu^{2+}-O^{2-}-Cu^{2+}, are the catalytic centers of NO decomposition when reduced to the Cu^{+}--Cu^{+} by the removal of bridged oxygen. There are a number of experimental evidences [Anpo et al., 1997; Beutel et al., 1996; Da Costa et al., 2002; Groothaert et al., 2003; Kuroda and Iwamoto, 2004; Kuroda et al., 1999; Lei et al., 1995; Lee, 2004; Modén et al., 2002; Sakany et al., 1992; Yan et al., 1996] supporting that oxygen-bridged Cu^{2+}-dimer ions are available on the high Cu-exchanged zeolite catalysts in the oxidized state. In a recent paper [Lee, 2004], it was experimentally demonstrated that Cu^{2+}-dimer ions over Cu-ZSM-5 catalyst were involved in the decomposition of NO to N_2 as catalytic centers via a cyclic redox process. The loaded copper on the catalysts in oxidized state was found to be present as isolated Cu^{2+}, Cu^{2+}-O^{2-}-Cu^{2+} and CuO, and the molar composition of each species on a catalyst was quantitatively determined. It was also revealed that the mol fraction of Cu_d (copper involved in the Cu^{2+}-O^{2-}-Cu^{2+} species of a catalyst) was higher for the catalysts based on the ZSM-5 with the lower ratio of Si to Al_f, and increased at the sacrifice of the isolated Cu^{2+} with increasing level of copper loading to a ZSM-5, ensuring that the Cu^{2+}-O^{2-}-Cu^{2+} species could be formed between the two isolated Cu^{2+} in close proximity.

Regarding the NO decomposition mechanism based on the Cu^{2+}-dimer species as catalytic centers, it was suggested that the removal of the bridged oxygen from the Cu^{2+}-O^{2-}-Cu^{2+} led to the reduction of Cu^{2+} to the Cu^{+}--Cu^{+} ion sites, on which NO adsorbs initiating the decomposition catalysis, and that two adsorbed NO molecules on the Cu^{+}--Cu^{+} species reacted to form N_2O as a reaction intermediate to product N_2, resultantly leaving the Cu^{2+}-O^{2-}-Cu^{2+} on surface [Kuroda and Iwamoto, 2004; Modén et al., 2002a]. In the kinetic expression like a Langmuir-Hinshelwood-Hougen-Watson (LHHW) rate equation, provided that the rate-determining step is relevant to N_2O formation, the kinetic term in the numerator would be expressed by the second order with respect to the NO pressure, while the adsorption group of the denominator would consist of such kinds of ad-species on the active sites as atomic oxygen, molecular oxygen, NO, NO_2, N_2O, and/or NO_3, as proposed by Modén et al. [2002a].

For the Cu-ZSM-5 catalyzed NO decomposition, it was commonly observed that the rate of N_2 formation was severely inhibited by the presence of O_2 in gas phase [Modén et al., 2002a; Li and Hall, 1991], and maximized at temperature around 500 °C [Modén et al., 2002a; Li and Hall, 1991; Yokomichi et al., 2000; Tomasic et al., 1998]; however, the reasons for these are not well understood. To resolve such implication involved in the Cu-ZSM-5 catalyzed NO decomposition, thermodynamic information on the activation energy of N_2 formation and the adsorption enthalpies of NO or O_2 to the reduced Cu^{+}-dimers is indispensable. As prerequisite to this, a kinetic expression based on the normalized rate of NO decomposition to the active Cu ion dimer sites of a Cu-ZSM-5 catalyst should be obtained. In this paper, LHHW-type kinetics of NO decomposition over Cu-ZSM-5 was established using the Cu_d-normalized rate of NO

†To whom correspondence should be addressed.
E-mail: dklee@gwangju.ac.kr

Table 1. Cu-ZSM-5 catalysts prepared and characterized [Lee, 2004]

	Cu(116)-Z(14.7)	Cu(76)-Z(14.7)	Cu(262)-Z(29)	Cu(156)-Z(29)
μmol Cu[a]/g	521	352	611	354
μmol Cu_d[b]/g	198	113	220	106

[a]Total amount of the loaded copper per a gram catalyst.
[b]Amount of copper species in the oxidized dimeric form, $(Cu\text{-}O\text{-}Cu)^{2+}$, per a gram catalyst.

decomposition to N_2 from the kinetic experiment over a Cu-ZSM-5 catalyst of which the catalytic amount of the active Cu^{2+}-dimers had been determined. And, thermodynamic data of reaction activation energy and enthalpies of adsorption/desorption of NO and O_2 from/to the active site were obtained and discussed with respect to the observed implication in the reaction.

EXPERIMENTAL

1. Catalyst Preparation

Cu-ZSM-5 catalysts with different Cu loadings, as listed in Table 1, were prepared by ion exchange of Cu^{2+} ions into Na-ZSM-5. Further details of catalyst preparation and characterization can be found elsewhere [Lee, 2004]. For the notation of catalysts in Table 1, the numbers in parentheses following Cu and Z indicate the %Cu exchange level (%Cu EL) and the Si/Al_f, respectively. The %Cu EL is defined as two hundred times the atomic ratio of total copper to Al_f of ZSM-5, i.e., 100% corresponds to one Cu^{2+} exchanged per two Al_f atoms.

2. Measurement of NO Decomposition Reaction Rate

Two kinds of reactors were used for the determination of the catalytic reaction rate. First, a multitube reactor designed for evaluating the catalysts up to eight samples simultaneously at the same reaction condition was used for the determination of activities of all the prepared catalysts. The reactor consisted of eight stainless steel tubes (inner diameter 2.5 mm) in parallel, which were inserted within a stainless steel block in order to ensure uniform temperatures. About 50 mg of fresh catalyst samples was loaded to each of the tube reactors. The catalysts in the reactors were pretreated for the reduction with 30 cm^3/min of He (UHP grade) for 2 h at 550 °C before their exposure to the reactant gas. The reactant gas was the mixture of 1.0% NO/9.98% Ar/89.02% He (1% NO gas). The 1% NO gas flow through each reactor was controlled to 60 cm^3/min (0.05 g/(cm^3/min)). Exit streams at steady state were routed to an online mass spectrometer (MS, MKS Instruments) one by one using an eight-port switching valve (Valco) for analysis.

Next, in order to obtain the kinetic data of NO decomposition over the catalyst Cu(116)-Z(14.7), reaction experiments were conducted using a quartz reactor with a porous quartz frit, over which 50 mg of catalyst sample was so evenly supported to give a differential reactor with shallow bed with a height less than 5 particle diameters. The catalyst was pre-reduced by the same procedure as above. Experiments were conducted at ambient pressure at temperatures, 400-600 °C, and the feed concentrations of NO were adjusted to 0.2, 0.34, 0.6, and 1% by mixing pure He and the 1% NO gas. The flow rate of total feed gas at a specified concentration of NO was changed by using a mass flow controller to give space time, 0.01-0.05 g-cat s/cm^3. Monitored species by the MS were as follows: He (4 amu), O (16), H_2O (18), NO (30), N_2 (28), O_2 (32), Ar (40), N_2O (44) and NO_2 (36). In order to calibrate the MS, a calibration gas mixture containing 0.05% N_2, 0.05% O_2, 0.05% N_2O, 10% Ar (used as internal standard) and 89.85% He was used. For the calibration of NO_2 MS signal, a mixed gas of 0.05% NO_2/9.94% Ar/90.01% He was used.

Table 2. Mechanism of NO decomposition over Cu-ZSM-5

Formation of N_2O on a reduced Cu-dimer	
1. $NO+[Cu^+\text{--}Cu^+] \Leftrightarrow [Cu^+(NO)\text{--}Cu^+]$	
2[a]. $NO+[Cu^+(NO)\text{--}Cu^+] \rightarrow [Cu^{2+}\text{-}O^{2-}\text{-}Cu^{2+}] + N_2O$	(rate determining step, RDS)
Formation of N_2O on the two oxidized Cu-dimers in vicinity	
3. $NO+[Cu^{2+}\text{-}O^{2-}\text{-}Cu^{2+}] \Leftrightarrow [Cu^{2+}(NO)\text{-}O^{2-}\text{-}Cu^{2+}]$	
4. $[Cu^{2+}(NO)\text{-}O^{2-}\text{-}Cu^{2+}] \Leftrightarrow [Cu^+(NO_2)\text{--}Cu^+]$	(activated above 50 °C)
5. $NO+[Cu^+(NO_2)\text{--}Cu^+] \Leftrightarrow [Cu^+(NO_2)\text{--}Cu^+(NO)]$	
6. $[Cu^+(NO_2)\text{--}Cu^+(NO)]\text{--}[Cu^+(NO)\text{--}Cu^+(NO_2)] \rightarrow 2Cu^+(NO_2)+[Cu^{2+}\text{-}O^{2-}\text{-}Cu^{2+}]+N_2O$	(swift even at RT)
Formation of N_2 and/or O_2 on a Cu-dimer	
7. $N_2O+[Cu^+\text{--}Cu^+] \rightarrow [Cu^{2+}\text{-}O^{2-}\text{-}Cu^{2+}]+N_2$	(swift even at RT)
8. $N_2O+[Cu^{2+}\text{-}O^{2-}\text{-}Cu^{2+}] \rightarrow [Cu^+\text{--}Cu^+]+N_2+O_2$	(activated above 300 °C)
Formation of O_2 on the two oxidized Cu-dimers in vicinity	
9. $2[Cu^{2+}\text{-}O^{2-}\text{-}Cu^{2+}] \Leftrightarrow 2[Cu^+\text{--}Cu^+]+O_2$	
Formation of NO_2 involving the reduction of a Cu-dimer	
10. $[Cu^+(NO_2)\text{--}Cu^+] \rightarrow [Cu^+\text{--}Cu^+]+NO_2$	(activated above 250 °C)

[a]The reaction in step 2 can be divided into the two elementary steps as follows:
2a. $NO+[Cu^+(NO)\text{--}Cu^+] \Leftrightarrow [Cu^+(NO)\text{--}Cu^+(ON)]$ (quasiequilibrated, RDS)
2b. $[Cu^+(NO)\text{--}Cu^+(NO)] \rightarrow [Cu^{2+}\text{-}O^{2-}\text{-}Cu^{2+}]+N_2O$ (swift even at RT)

DERIVATION OF KINETIC EXPRESSION

1. Backgrounds of the Proposed Reaction Mechanism

The reaction mechanism proposed in this study is summarized in Table 2. As briefly mentioned in the introduction, as far as the Cu^{2+}-dimers are regarded as catalytic centers, there is little disagreement on that the reaction of two adsorbed NO molecules on a Cu^{+}-dimer species led to the formation of N_2O as a precursor of N_2, leaving the resultant Cu^{2+}-O^{2-}-Cu^{2+} species on surface (elementary reaction steps: 1-2). The Cu^{+}(NO) ad-species on the surface was evidenced by IR measurement [Konduru and Chuang, 1999], and the formation of N_2O prior to N_2 was experimentally observed [Modén et al., 2002a]. One NO-adsorbed dimer species, Cu^{+}(NO)--Cu^{+}, would be equilibrated with the pressure of NO in gas phase, as represented in step 1. If the reaction between the two NO-adsorbed Cu^{+} species in a dimer leading to N_2O formation (step 2b) is fast enough to not permit the desorption of any NO, the rate of N_2O formation would be governed by that of step 2a, the second adsorption of NO to the Cu^{+}(NO)--Cu^{+}.

Fig. 1 shows the swiftness of the reaction forming N_2O even at room temperature. This result was obtained at room temperature by switching the gas flow (100 cm^3/min) over the reduced catalyst sample of Cu(116)-Z(14.6) in a quartz reactor from He to the gas of 0.464% NO/Ar/He. For the reduction of the catalyst, the sample stored after drying was thermal-treated at 550 °C in He flow for 2 h and cooled to room temperature. In Fig. 1, the advent of Ar in MS indicates the beginning of NO adsorption onto the catalyst, and that of NO indicates that such NO adsorption is near an equilibrium state. Just before reaching the equilibrium state of NO adsorption, the formation of N_2O and N_2 in more than discernable amounts is observed, ensuring the swiftness of step 2b. This result suggests that step 7 forming N_2 via N_2O adsorption to a reduced Cu-dimer is also a very swift process even at room temperature. Consequently, step 2 deserves to be regarded as the rate-determining step in the NO decomposition reaction to N_2.

As the other possible route of N_2O formation, there is a need to consider elementary steps 3 through 6 since experimental evidence for that is available, as shown in Fig. 6(A) of the previous paper [Lee, 2004]. It shows the turnover frequency (TOF) of the gases detected during the temperature-programmed surface reaction of NO (NO-TPSR) over the oxidized catalyst sample of Cu(116)-Z(14.7). As previously described [Lee, 2004], for the pre-oxidation, the catalyst sample was thermally treated using a gas mixture of 49% O_2/He (O_2 gas) at 500 °C for 2 h, and after that, the reactor was cooled to room temperature. Then, pure He was introduced instead of the O_2 gas in order to remove physisorbed oxygen on the catalyst. The fact that most of Cu-dimers over the catalysts after such a thermal oxidation existed as the Cu^{2+}-O^{2-}-Cu^{2+} species was evidenced by the temperature-programmed desorption (TPD) of O_2 in He flow [Lee, 2004]. For the NO-TPSR, the flow of He was switched to the flow (100 cm^3/min) of 0.464% NO/Ar/He over the catalyst, and after the NO-adsorption equilibration at room temperature, the reactor temperature was raised by 10 °C/min, various kinds of products appeared with increasing temperature. In this process, only N_2O was observed to be formed in a significant amount at a relatively low temperature region, followed by the NO_2 formation at temperatures above 250 °C. It should be noted that N_2O appearing at temperatures lower than 250 °C should have resulted from a different route than the reaction steps 1-2, because of the scarcity of the Cu^{+}--Cu^{+} species on surface due to the preoxidation. In reference to the suggestion of Beutel et al. [1996] that the adsorption of two NO onto an oxidized Cu-dimer resulted in a Cu^{+}-NO and a $(Cu\text{-}NO_2)^{+}$ complex, steps 3-5 were established. Reaction step 4 was introduced because the adsorption of NO onto an oxidized Cu-dimer was not likely to directly lead to the reduction of the Cu^{2+} as the $Cu^{+}(NO_2)$--Cu^{+} at room temperature. During the period of NO-adsorption equilibration at room temperature over the oxidized catalyst, any discernable amount of N_2O or N_2 was not detected. As shown in Fig. 6(A) of the previous paper [Lee, 2004], the formation of N_2O started at temperature above 50 °C, indicating that a little extent of activation energy was required for the reaction step 4. As described in step 6, if two of the resultant Cu^{+}(NO)--$Cu^{+}(NO_2)$ species are placed so close for the two Cu^{+}(NO) species to associate as a dimer, this results in the formation of N_2O, resultantly leaving a new Cu^{2+}-O^{2-}-Cu^{2+} with two separately existing $Cu^{+}(NO_2)$ species. This reaction may be possible for Cu-ZSM-5 over which the copper species involved in the dimers are highly clustered, like the case of the thermal recombined formation of O_2 from the two vicinal Cu^{2+}-O^{2-}-Cu^{2+} species, as previously reported [Lee, 2004, 2005]. Before the desorption of NO_2, this process would be continued with concurrent formation of N_2O until quite a large amount of the Cu^{2+}-O^{2-}-Cu^{2+} species transformed to $Cu^{+}(NO_2)$ species. The resulting species of $Cu^{+}(NO_2)$ on surface observed to desorb at temperatures above 250 °C. This desorption of NO_2 can be resultantly thought as a reduction process of the oxidized Cu^{2+}-dimers, as described by step 10. In actual NO decomposition condition where O_2 is always prevailing, the reaction steps 3-6 would take charge of the formation of N_2O to some extent, but small as compared to the steps 1-2 because of the low-efficiency of the process needing four active Cu ions.

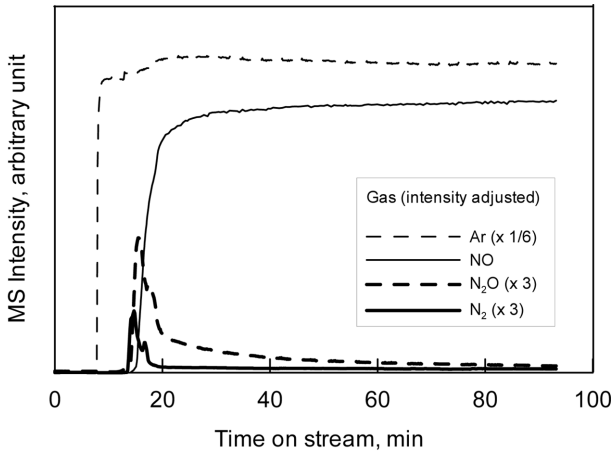

Fig. 1. Formation of N_2O and N_2 at room temperature during the flow of 0.464% NO/Ar/He over the pre-reduced catalyst of Cu(116)-Z(14.7).

As routes of N_2 formation from N_2O, except for the elementary step 7 discussed prior in its swiftness, step 8 needs to be considered referring to Fig. 5(A) of the previous paper [Lee, 2004]. It shows the TOF of the gases detected during the N_2O-TPSR over the oxidized catalyst sample of Cu(116)-Z(14.7). Pre-oxidation treatment was the same as for the NO-TPSR, and gas of 0.1% N_2O/He was

used for the N_2O-TPSR. At temperatures above 300 °C, N_2O observed to decompose over the oxidized catalyst into N_2 and O_2. Up to about 360 °C, the TOFs of N_2 and O_2 evolved were practically equivalent to each other, indicating that the reaction step 8 was working. According to the proposal of Kuroda and Iwamoto [2004] for N_2 formation via the adsorption of N_2O onto an oxidized Cu-dimer site, Cu^{2+}-(O^--O^-)-Cu^{2+} species remain on surface; however, this figure suggests a prompt desorption of O_2 in parallel with N_2 at temperatures above 300 °C. In respect of the removal of the Cu^{2+}-bridged atomic oxygen, step 8 as well as step 10 can be thought of as an efficient reduction process for oxidized dimers as compared to step 9, requiring two vicinal oxidized Cu^{2+}-dimers.

2. Kinetic Rate Equation

To establish an LHHW-type kinetic rate equation, based on the mechanism in Table 2, the kinds of prevailing ad-species on the catalytic sites are to be determined. According to the above discussion on the reaction mechanism, candidate ad-species would be [Cu^+--Cu^+], [Cu^{2+}-O^{2-}-Cu^{2+}], [Cu^+(NO)--Cu^+], and [$Cu^+(NO_2)$--Cu^+], termed briefly as [*], [O*], [NO*], and [NO_2^*], respectively, to represent their site-occupying mol fractions. If the reaction rate could be expressed on the basis of one mol of the Cu_d species involved in the Cu^{2+}-dimer sites, the site balance would be given by

$$1=[*]+[O*]+[NO*]+[NO_2^*] \quad (1)$$

As discussed above, step 2 is regarded as the rate-determining step for the N_2 formation. The Cu_d-normalized reaction rate of N_2 formation, r (mmol-N_2/mol-Cu_d/s), is represented by

$$r=k_2P_{NO}[NO*] \quad (2)$$

where k_2 (mmol-N_2/mol-Cu_d/kPa-NO/s) is a rate constant in the reaction step 2, and P_{NO} is the NO pressure in kPa. The equilibrium relationships in steps 1, 3 and 9 lead to Eqs. (3), (4) and (5), respectively:

$$[NO*]=K_1P_{NO}[*] \quad (3)$$

$$[NO_2^*]=K_3P_{NO}[O*] \quad (4)$$

$$[O*]=K_9^{-0.5}P_{O_2}^{0.5}[*] \quad (5)$$

where K_1 (1/kPa), K_3 (1/kPa) and K_9 (kPa) are the adsorption equilibrium constants in the steps, 1, 3 and 9. By substituting Eqs. (3)-(5) into Eq. (1), and replacing [NO*] of Eq. (2) with Eq. (3), and after some arrangements, a final equation for the rate of N_2 formation is obtained:

Table 3. Parameters for the kinetics of NO decomposition over Cu(116)-Z(14.7)

Temperature, °C	k_{app}^a	K_1^b, 1/kPa	K_3^b, 1/kPa	K_9^{-1}, 1/kPa	k_2^c	SD[d]
400	159.2	9.34	1.77	10404	17	0.064
450	162.6	2.97	0.41	4516	55	0.079
500	94.4	(0.65)	(0.12)	1233	145	0.195
550	30.3	(0.12)	(0.04)	243	252	0.122
600	14.9	(0.03)	(0.02)	124	496	0.150

[a] mmol-N_2/mol-Cu_d/s/kPa^2

[b] Numeric values in parentheses were taken to get straight lines for all data in the Arrhenius plots shown in Fig. 3.

[c] k_2 (mmol-N_2/mol-Cu_d/s/kPa) = k_{app}/K_1

[d] Standard deviation of the calculated rate data from the experimental.

$$r=\frac{k_{app}P_{NO}^2}{D} \quad (6)$$

where k_{app} (mmol-N_2/mol-Cu_d/kPa^2/s), an apparent rate constant of N_2 formation from the NO decomposition reaction, and the denominator D, are given by, respectively

$$k_{app}=k_2K_1 \quad (7)$$

$$D=1+K_9^{-0.5}P_{O_2}^{0.5}+K_1P_{NO}+K_3K_9^{-0.5}P_{NO}P_{O_2}^{0.5} \quad (8)$$

RESULTS AND DISCUSSION

1. Determination of Kinetic Parameters

Table 3 lists the values of the parameters in Eq. (6) and k_2 calculated by using Eq. (7), which were obtained through a multi-nonlinear regression for the rate data expressed as mmol-N_2 formation per mol-Cu_d per second at the reaction temperatures 400-600 °C. For the catalyst, Cu(116)-Z(14.7), the amount of Cu_d was determined to 198 μmol per a gram of the catalyst [Lee, 2004], as shown in Table 1. At each temperature level, a rate data set consisting of 20 points were obtained by varying the reactor space-time of feed gas and the feed pressure of NO. The pressure of NO in the catalyst bed was calculated from the feed NO conversion to the MS-measured N_2, N_2O and NO_2, and that of O_2 was based on the MS-measured intensity of O_2.

The rate data at 400 and 450 °C were fitted very well to Eq. (6),

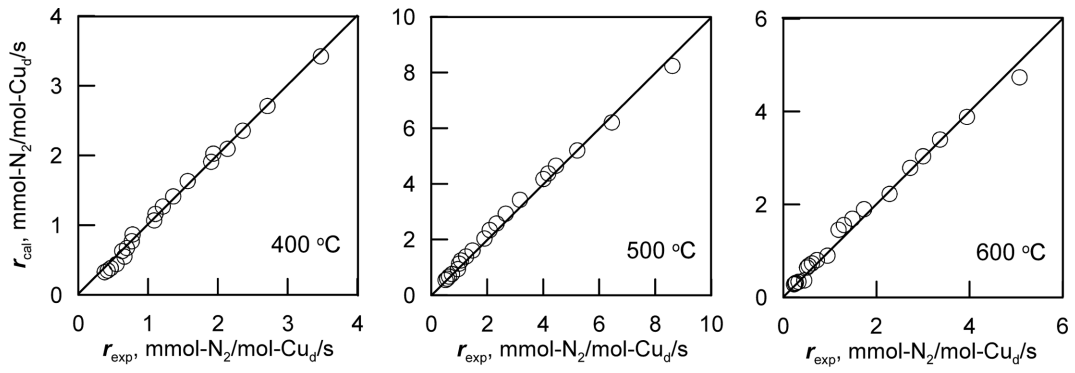

Fig. 2. Parity plots of the calculated rate of N_2 formation against the experimental at temperatures 400, 500, and 600 °C.

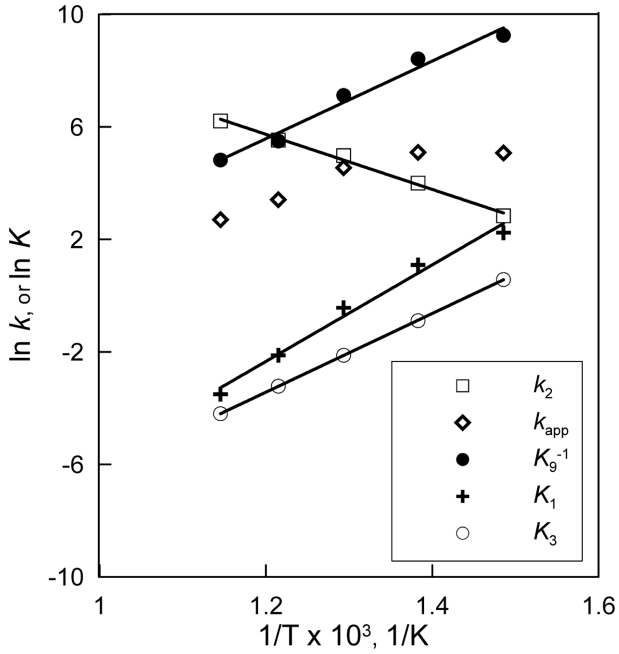

Fig. 3. Arrhenius plot for the kinetic parameters in Table 3.

giving each of the parameter values listed in Table 3. However, for the data set at 500 °C and the above temperatures, it was not possible to obtain the values of parameters K_1 and K_3 with adequate physical significance from the regression due to their so much small values as compared to $K_9^{-0.5}$. So, K_1 and K_3 values in parentheses in Table 3 were so properly taken that all the data of K_1, k_2 and K_3 could be represented as linearly as possible on the Arrhenius plot. With these pre-set values of K_1 and K_3, the values of K_{app} and K_9 were obtained from the regression of the rate data using Eq. (6). Fig. 2 shows the parity plot of the calculated rate of N_2 formation using Eq. (6) with the parameters in Table 3 against the experimental at typically 400, 500 or 600 °C. Fig. 3 shows the Arrhenius plots for each of the parameters determined. In view of good correspondence between the rates of calculated and experimental, and the linear Arrhenius relationships of the parameters, the kinetic equation given by Eq. (6) with the parameters determined could be thought to reasonably depict the reaction kinetics of NO decomposition to N_2 over the Cu-dimers as catalytic centers.

Table 4. Reaction activation energy and enthalpy of adsorption

E_{A_2} (activation energy of the reaction in step 2), kcal/mol	19.5
ΔH_1 (heat of adsorption of NO to * in step 3), kcal/mol	−34.1
ΔH_3 (heat of adsorption of NO to O* in step 3), kcal/mol	−27.8
ΔH_9 (heat of dissociative adsorption of O_2 in step 9), kcal/mol	−27.4
E_{A_app} (apparent activation energy=$E_{A\_2}+\Delta H_1$), kcal/mol	−14.6

2. Enthalpies of the Adsorption of NO and O_2 onto the Cu-Dimers

The reaction activation energy and the enthalpies of adsorption calculated from the Arrhenius relationship shown in Fig. 3 are summarized in Table 4. The adsorption of NO onto a Cu^+ in the reduced Cu^+-dimer accompanies the exothermic heat of adsorption of 34.1 kcal/mol. This value is closely correspondent to the calculated result, 34.4 kcal/mol, by Yokomichi et al. [2000]. In this sense, the K_1 values pre-set in the determination of the kinetic parameters at 500 °C and above temperatures and the resultant k_2 may be thought as feasible. The relatively high value of ΔH_1 indicates the tendency of NO adsorption less favored at higher temperatures. The exothermic heat of adsorption of NO onto a Cu^{2+} in the oxidized Cu^{2+}-dimer is estimated as 27.8 kcal/mol, and that of dissociative adsorption of O_2 onto the two reduced Cu^+-dimers is 27.4 kcal/mol. From the viewpoint of adsorption equilibrium, larger heat of adsorption for an adsorbate means its higher tendency to desorb from the adsorbent as temperature increases. So, the thermal desorption of NO_2 and O_2 in sequence, with peak temperatures 375 and 395 °C, respectively, during the NO-TPSR shown in Fig. 6(A) of the previous paper [Lee, 2004] is closely related to these enthalpy values of adsorption. In Eq. (8), the Cu-dimer fractions of [NO_2*] and [O*] are calculated by $K_3K_9^{-0.5}P_{NO}P_{O2}^{0.5}/D$ and $K_9^{-0.5}P_{O2}^{0.5}/D$, respectively. Their temperature dependences are therefore related to the magnitude of enthalpies, $(-\Delta H_3)+(-\Delta H_9)/2$ and $(-\Delta H_9)/2$, respectively, each giving 41.5 and 13.7 kcal/mol. Such enthalpy difference is well reflected by the sequential desorption of NO_2 and O_2 with increasing temperature with a peak temperature difference about 20 °C in Fig. 6(A) of the previous paper [Lee, 2004].

3. Kinetic Effects of Temperature, P_{O2} and P_{NO}

Fig. 4 shows the change in the fractional coverage of ad-species on the Cu-dimer sites as [O*], [NO*], and [NO_2*] including the

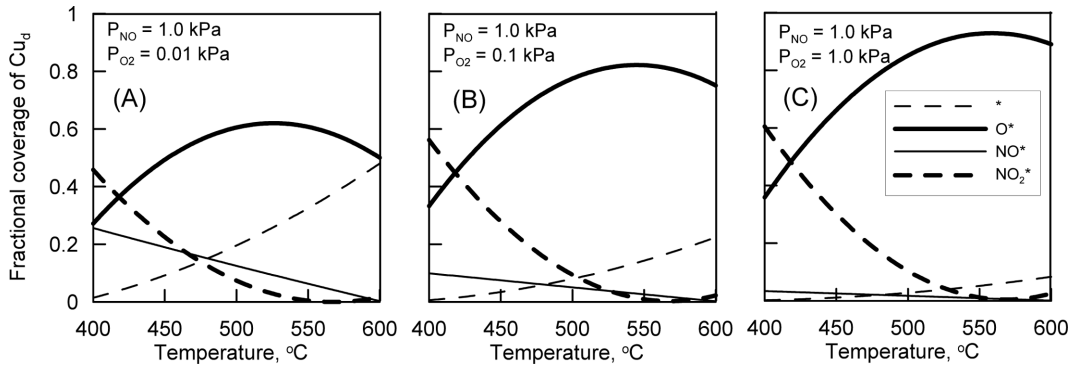

Fig. 4. Change of the fraction coverage of the Cu-dimer sites with temperature and O_2 pressures (A): 0.01, (B): 0.1, and (C): 1.0 kPa under a constant pressure of NO at 1.0 kPa.

vacant [*] with temperature at P_{NO}=1 kPa and different levels of P_{O2}. As expected by the enthalpy difference between [NO_2*] (41.5 kcal/mol) and [NO*] (34.1 kcal/mol), the coverage of the former decreases more rapidly than that of the latter as temperature increases. This is consistent with the result of in-situ IR study for the NO-TPSR over Cu-ZSM-5 by Konduru and Chuang [1999], reporting that the IR intensity of $Cu^{2+}O^{-}$(NO) disappeared rapidly with concurrent desorption of NO_2 as temperature increased. As listed in Table 5, free energies calculated from the adsorption equilibrium constants at different temperatures indicate that the adsorption of NO onto [Cu^{+}--Cu^{+}] and [Cu^{2+}-O^{2-}-Cu^{2+}] is not thermodynamically favored at temperatures above from 500 and 450 °C, respectively, while the dissociative adsorption of O_2 onto [Cu^{+}--Cu^{+}] is highly favored all over the temperature. Therefore, even under the presence of O_2 in a very low pressure like P_{O2}=0.01 kPa, as shown in Fig. 4(A), the site-fraction of [O*] is predominant over the others mostly throughout the temperature experimented. The presence of O_2 in higher pressures leads to higher site-fraction of [O*], as shown in Fig. 4(B) and 4(C). In this regard, severe O_2 inhibition reported [Modén et al., 2002a; Li and Hall, 1991] on the rate of the NO decomposition to N_2 over Cu-ZSM-5 catalysts can be well understood. The rate of N_2 formation calculated by Eq. (6) at conditions including the P_{NO} and P_{O2} examined in Fig. 4 is shown in Fig. 5(A). The rate of N_2 formation appears to be highly inhibited by O_2 even at very low pressure.

Table 5. Free energy in the adsorption equilibria over Cu-dimers

Temperature, °C	ΔG[a], kcal/mol-adsorbate		
	Step 1	Step 3	Step 9 (reversed)
400	−3.0	−0.8	−12.4
450	−1.6	1.3	−12.1
500	0.7	3.3	−10.9
550	3.5	5.3	−9.0
600	6.1	6.8	−8.4

[a]ΔG=−RT lnK, where K is equal to K_1, K_3 or K_9^{-1} in Table 3.

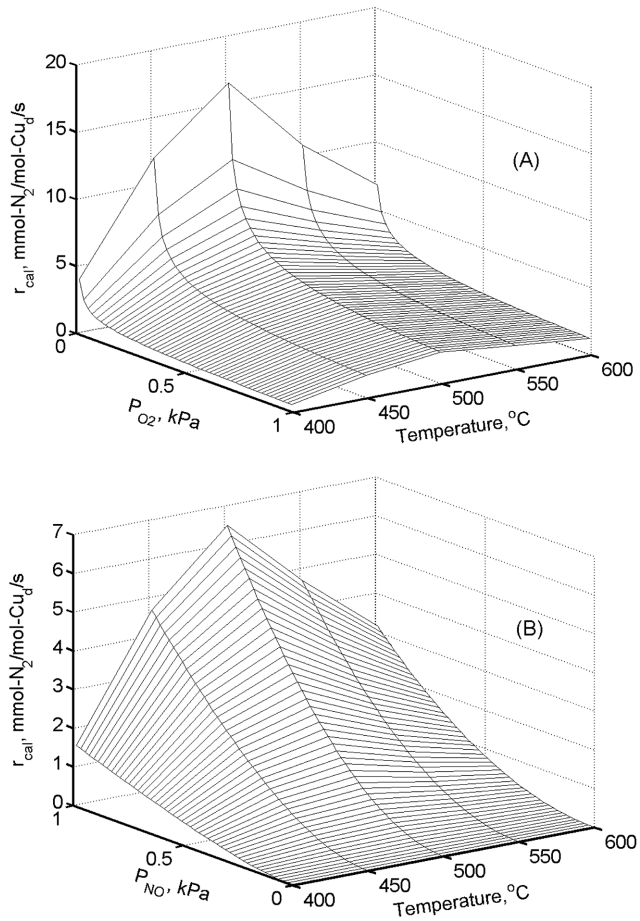

Fig. 5. (A) The dependence of the calculated rate of N_2 formation on temperature and O_2 pressure at P_{NO}=1 kPa, and (B): that on temperature and NO pressure at P_{O2}=0.1 kPa.

Fig. 5(A) demonstrates also that the calculated rate of N_2 formation is maximized at temperature around 500 °C. Such a temperature dependence of the catalytic activity was commonly observed in the NO decomposition reaction over Cu-ZSM-5 catalysts [Modén et al., 2002a; Li and Hall, 1991; Yokomichi et al., 2000; Tomasic et al., 1998]. In view of the above discussion on NO adsorption, it can be thought that this unusual activity pattern with increasing temperature is attributed to the relatively large enthalpy of adsorption NO onto the [Cu^{+}--Cu^{+}] site as compared to the reaction activation energy in step 2, as the values given in Table 4. As a result, apparent activation energy (E_{A_app}=−14.6 kcal/mol) appears negatively in the NO decomposition reaction, suggesting that the apparent rate constant given by Eq. (7) decreases with the increase of temperature.

Fig. 5(B) shows the dependence of the calculated rate of N_2 formation on the pressure of NO and temperature at P_{O2}=0.1 kPa. The apparent reaction order with respect to the P_{NO} was calculated to 1.75, 1.91, 1.97, 1.99 and 2.0 at temperatures 400, 450, 500, 550 and 600 °C, respectively. This indicates that at higher temperatures above 500 °C, the dimer site-coverage of [NO*] becomes negligible to have no contribution to the denominator term given by Eq. (8).

4. Activation Energy of Dissociative Adsorption of O_2 onto the Reduced Cu-Dimers

Activities of the catalysts of Table 1, determined in the experiments using the multitube reactor, showed the same temperature

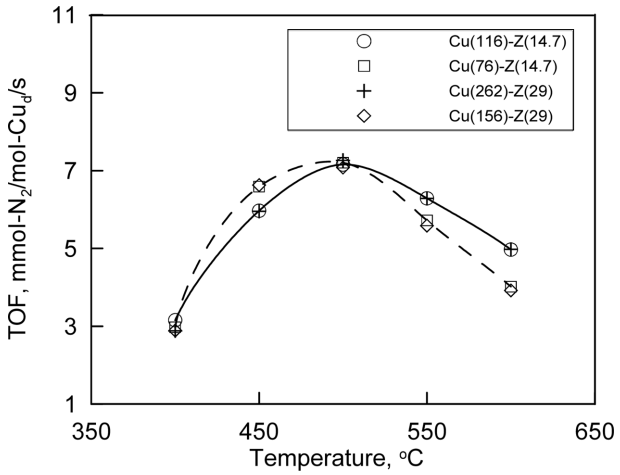

Fig. 6. Rate of N_2 formation in terms of the TOF based on the Cu_d of the catalysts.

dependency as observed in Fig. 5(A). Temperature dependence of the rate of N_2 formation in terms of the TOF based on total amount of Cu loaded was shown in Fig. 1 of the previous paper [Lee, 2004]. Fig. 6 shows the rate in terms of the TOF based on the Cu_d of the catalysts. It is interesting that the catalysts showing different catalytic activities among them in the TOF based on the total Cu can be classified into two groups of the same activity in the TOF based on the Cu_d: One group of Cu(116)-Z(14.7) and Cu(262)-Z(29), and the other of Cu(76)-Z(14.7) and Cu(156)-Z(29), as shown in Fig. 6. The two catalysts in each group are similar to each other in their mol amounts of Cu_d per a gram catalyst, as given in Table 1, taking it for granted that their Cu_d-normalized TOFs appear nearly same when considering the Cu-dimers as active centers. Catalysts in the former group are about twice more than the latter in the amounts of Cu_d/g. Another interesting point in Fig. 6 is that the catalysts with higher amounts of Cu_d/g are less active at lower temperature than those with lower amounts of Cu_d/g. This may result from the difference between the two groups of catalysts in the degree of O_2-inhibition effect at low temperatures. In a recent paper [Lee, 2005], it was revealed that the activation energy ($E_{A\_O2\_des}$) for the thermal O_2 desorption via a recombination of atomic oxygen from the Cu^{2+}-O^{2-}-Cu^{2+} sites decreased linearly with increasing Cu_d/g, as listed in Table 6. With the values of $E_{A\_O2\_des}$, it is possible to obtain the activation energy ($E_{A\_O2\_ads}$) for the dissociative adsorption of O_2 onto the two vicinal [Cu^+--Cu^+] sites using the following relationship:

$$E_{A\_O_2\_ads}=E_{A\_O_2\_des}-(-\Delta H_9) \quad (9)$$

As listed in Table 6, the catalysts with higher amounts of Cu_d/g need much less activation energies for the dissociative adsorption of O_2 than those with lower amounts of Cu_d/g. Accordingly, at low temperatures around 450 °C, the former catalysts are expected to severely suffer from higher dimer site-fraction of [O*] in comparison with the latter, by which the former catalysts appear less active than the latter, as shown in Fig. 6. At higher temperatures where the difference in the $E_{A\_O2\_ads}$ between the two groups of catalysts does not bring any significant effect, the former catalysts with lower $E_{A\_O2\_des}$ become more active than the latter with higher $E_{A\_O2\_des}$.

On the mechanism proposed in Table 2, there are three different ways of atomic oxygen removal from the [Cu^{2+}-O^{2-}-Cu^{2+}]: step 8, step 9, and the step 10 through steps 3-4. From the TOF profile of NO_2 desorption in the NO-TPSR shown in Fig. 6(A) of the previous paper [Lee, 2004], the activation energy ($E_{A\_NO2\_des}$) for NO_2 desorption was obtained as 22.3 kcal/mol at the temperature span (250-300 °C) of initial desorption. And, the activation energy ($E_{A\_O2\_form}$) for O_2 formation in the N_2O-TPSR shown in Fig. 5(A) of the previous paper [Lee, 2004] was 18.9 kcal/mol at temperature region 300-350 °C where N_2 and O_2 are evolved in the same TOF. These lower activation energies over the catalyst of Cu(116)-Z(14.7) as compared to that (35.3 kcal/mol) for the thermal recombined desorption of O_2 indicates the readiness of the atomic oxygen removal via step 8 and step 10 relative to via step 9. Considering the prevailing inhibition effect by gas phase oxygen on the kinetic rate during NO decomposition, step 9 should be regarded as an equilibrated route for the dissociative adsorption of O_2 onto the Cu^+--Cu^+ sites, whereas the reduction of oxidized Cu^{2+}-dimers to Cu^+--Cu^+ is mostly carried out via step 8 and step 10.

SUMMARY

Cu_d-normalized reaction rate of N_2 formation in the Cu-ZSM-5 catalyzed NO decomposition was well represented by the proposed reaction mechanism-based kinetic model. The numerator term in the kinetic equation was expressed as $k_{app}P^2_{NO}$ by assuming the second NO adsorption onto a molecule of NO-adsorbed Cu^+-dimer, [NO*], as the rate-determining step for the N_2 formation, and the denominator consisted of the adsorption terms of [O*], [NO*], [NO_2*], and [*] as the vacant Cu^+-dimer. It was characteristic for the NO decomposition reaction over Cu-ZSM-5 that the enthalpy of the adsorption of NO ($\Delta H=-34.1$ kcal/mol) onto the [*] site was higher than that ($\Delta H=-27.8$ kcal/mol) onto the [O*], or that ($\Delta H=-27.4$ kcal/mol) of the dissociative adsorption of O_2 onto the two [*] sites in neighbor. The adsorption of NO onto the sites of [*] and [O*] was not thermodynamically favored at temperatures above 500 and 450 °C, respectively. However, the dissociative adsorption of O_2 onto the [*] site was always favored throughout the temperature of 400-600 °C, and resultantly, the rate of N_2 formation appeared to be highly inhibited by O_2 even at very low pressure. The unusual catalytic behavior showing a maximum activity around 500 °C was attributed to the relatively large enthalpy of NO adsorption onto the [*] as compared to that of the reaction activation energy (19.5 kcal/mol), resultantly giving the negative apparent activation energy ($E_{A\_app}=-14.6$ kcal/mol). The catalysts with higher amounts of Cu_d/g were analyzed to need much less activation energies (4.6-7.9 kcal/mol) for the dissociative adsorption of O_2 than those (21.0-22.5 kcal/mol) with lower amounts of Cu_d/g. It was believed that the [O*] on the catalyst maintained in equilibrated state by the dissociative adsorption of O_2 onto the [*] sites while the reduction of [O*] to [*] seemed to be mostly carried out via the reaction of N_2O with [O*] and the adsorption of NO onto the [O*] followed by the desorption of NO_2.

ACKNOWLEDGMENT

The author expresses his deep thanks to Professor Enrique Iglesia and Mr. Björn Modén in the Ph. D course at the Department of Chemical Engineering, University of California, Berkeley for their

Table 6. Activation energy involved in the desorption/adsorption of O_2 over Cu-dimers

	Cu(116)-Z(14.7)	Cu(76)-Z(14.7)	Cu(262)-Z(29)	Cu(156)-Z(29)
$E_{A\_O2\_des}$[a], kcal/mol	35.3	48.4	32.0	49.9
$E_{A\_O2\_ads}$[b], kcal/mol	7.9	21.0	4.6	22.5

[a]Activation energy for the thermal recombined desorption of O_2 from the two [Cu^{2+}-O^{2-}-Cu^{2+}] species, from the reference [Lee, 2005].
[b]Activation energy for the dissociative adsorption of O_2 onto the two [Cu^+--Cu^+] species, calculated by Eq. (9).

kind help and discussion. It is acknowledged that the raw data of this paper were obtained from the author's experimental work in the Professor Iglesia's laboratory.

REFERENCES

Anpo, M., Matsuoka, M., Hano, K., Mishima, H., Ono, T. and Yamashita, H., "Photocatalytic decomposition of N_2O on Cu^+/Y-zeolite catalysts prepared by ion-exchange," *Korean J. Chem. Eng.*, **14**, 498 (1997).

Beutel, T., Sarkany, J., Lei, G-D., Yan, J. Y. and Sachtler, W. M. H., "Redox chemistry of Cu/ZSM-5," *J. Phys. Chem.*, **100**, 845 (1996).

Da Costa, P., Modén, B., Meitzner, G. D., Lee, D. K. and Iglesia, E., "Spectroscopic and chemical characterization of active and inactive Cu species in NO decomposition catalysts based on Cu-ZSM-5," *Phys. Chem. Chem. Phys.*, **4**, 4590 (2002).

Groothaert, M. H., Lievens, K., Leeman, H., Weckhuysen, B. M. and Schoonheydt, R. A., "An operando optical fiber UV-Vis spectroscopic study of the catalytic decomposition of NO and N_2O over Cu-ZSM-5," *J. Catal.*, **220**, 500 (2003).

Konduru, M. V. and Chuang, S. C., "Investigation of asdorbate reactivity during NO decomposition over different levels of copper ion-exchanged ZSM-5 using *in situ* IR technique," *J. Phys. Chem. B*, **103**, 5802 (1999).

Kuroda, Y. and Iwamoto, M., "Characterization of cuprous ion in high silica zeolites and reaction mechanisms of catalytic NO decomposition and specific N_2 adsorption," *Topics in Catal.*, **28**, 111 (2004).

Kuroda, Y., Kumashiro, R., Yoshimoto, T. and Nagao, M., "Characterization of active sites on copper ion-exchanged ZSM-5-type zeolite for NO decomposition reaction," *Phys. Chem. Chem. Phys.*, **1**, 649 (1999).

Lee, D. K., "Quantification and redox property of the oxygen-bridged Cu^{2+} dimers as the active sites for the NO decomposition over Cu-ZSM-5 catalysts," *Korean J. Chem. Eng.*, **21**, 611 (2004).

Lee, D. K., "Kinetic evaluation of mechanistic models for O_2 release from ZSM-5-supported [Cu^{2+}-O^{2-}-Cu^{2+}] ions by thermal reduction or chemical interaction with impinging N_2O molecules," *Catal. Lett.*, **99**, 215 (2005).

Lei, G. D., Adelman, B. J., Sarkany, J. and Sachtler, W. M. H., "Identification of Copper(II) and Copper(I) and their interconversion in Cu/ZSM-5 De-Nox catalysts," *Appl. Catal. B: Env.*, **5**, 245 (1995).

Li, Y. and Hall, W. K., "Catalytic decomposition of nitric oxide over Cu-zeolites," *J. Catal.*, **129**, 202 (1991).

Modén, B., Da Costa, P., Fonfe, B., Lee, D. K. and Iglesia, E., "Kinetics and mechanism of steady-state catalytic NO decomposition reactions on Cu-ZSM5," *J. Catal.*, **209**, 75 (2002a).

Modén, B., Da Costa, P., Lee, D. K. and Iglesia, E., "Transient studies of oxygen removal pathways and catalytic redox cycles during NO decomposition on Cu-ZSM5," *J. Phys. Chem. B*, **106**, 9633 (2002b)

Sakany, J., d'Itri, J. and Sachtler, W. M. H., "Redox chemistry in excessively ion-exchanged Cu/Na-ZSM-5," *Catal. Lett.*, **16**, 241 (1992).

Tomasic, V., Gomzi, Z. and Zrncevic, S., "Catalytic reduction of NO_x over Cu/ZSM-5 catalyst," *Appl. Catal. B: Env.*, **18**, 233 (1998).

Yan, J. Y., Lei, G-D., Sachtler, W. M. H. and Kung, H. H., "Deactivation of Cu/ZSM-5 catalysts for lean NOx reduction: characterization of changes of Cu state and zeolite support," *J. Catal.*, **161**, 43 (1996).

Yokomichi, Y., Yamabe, T., Kakumoto, T., Okada, O., Ishikawa, H., Nakamura, Y., Kimura, H. and Yasuda, I., "Theoretical and experimental study on metal-loaded zeolite catalysts for direct NO_x decomposition," *Appl. Catal. B: Env.*, **28**, 1 (2000).